

PAPER • OPEN ACCESS

Numerical simulation of lid-driven cavity flow of micropolar fluid

To cite this article: K Venkatadri *et al* 2018 *IOP Conf. Ser.: Mater. Sci. Eng.* **402** 012168

View the [article online](#) for updates and enhancements.



IOP | ebooks™

Bringing you innovative digital publishing with leading voices to create your essential collection of books in STEM research.

Start exploring the [collection](#) - download the first chapter of every title for free.

Numerical simulation of lid-driven cavity flow of micropolar fluid

K Venkatadri^{*1}, S Maheswari², C Venkata Lakshmi², V Ramachandra Prasad³

^{1,2}Department of Applied Mathematics, Sri Padmavati Mahila Visvavidyalayam, Tirupati-517502, A.P, India.

³Department of Mathematics, School of Advanced Sciences, VIT University, Vellore - 632014, Tamil Nadu, India.

*Corresponding author: venkatadri.venki@gmail.com

Abstract. Incompressible unsteady laminar flow of a micropolar fluid in a lid driven square cavity has been examined numerically with finite difference scheme. In this paper, we verify the code validation of Newtonian incompressible fluid ($K=0$) with standard benchmark problem in the literature and then proceed the present computation. The vorticity-stream function formulation of Navier-Stokes equations and angular momentum equation is solved by the Euler's explicit method. The effect of various values of Reynolds number (Re) and vortex viscosity parameter (K) of the flow characteristics is studied and discussed through several graphs.

1. Introduction

Fluid flows within or over the cavities has been several applications in the field of engineering. An incompressible fluid flow governing equations of cavity solvers increase the interest to study the benchmark driven flow problems in a cavity with moving top lid. Micropolar fluid is a major subject of theory of micropolar fluid. The micropolar fluid model is introduced by C.A Eringen [1]. Increased curiosity in mathematical modelling and numerical analysis of micro flows because it is an active research topic. There are several practical applications of micropolar fluid flows that include, Biofluids, animal blood, liquid crystals, colloidal suspensions, polymeric suspensions and so more. Many researchers studied lid driven cavity flow problem through numerically and experimentally [2-10] and their computed results are validated with ghia et al. [11]. Comparative study conducted by Hogan et al. [12] examined an idealized stenosis with blood flow. They are noticed that velocities profiles and flow patterns are similar in micropolar and the classical continuum theories. Sherief et al. [13] carried out perturbation technique on based investigation of creeping motion of micropolar fluid between two corrugated plates. Hari et al. [14] have studied natural convective incompressible micropolar fluid flows in between vertical walls under the influence of uniform magnetic field. Electromagnetics of micropolar fluid fundamentals are briefly presented by Chen et al. [15]. They examined the Balance laws of mass, energy, entropy angular and linear momentums, for Micropolar Fluid Dynamics (MFD) are integrated with Maxwell's equations. Ettwein et al. [16] have studied existence of weak solution for micropolar electrorheological. Muthu et al. [17] investigated oscillatory micropolar fluid flow behaviour in annular tube with different radius of out tube. Hogan et al. [18] developed finite element formulation of steady incompressible fluid flow with microstructure. They are exhibited for fully developed fluid flow through a straight tube and validated with an analytical solution.



In the current study, we compute the results of unsteady laminar incompressible micropolar fluid flows in a lid driven cavity with various values of Reynolds number. The finite difference technique is implemented for solving the linear momentum equation in the form of vorticity-streamfunction and angular momentum equations with the no-slip and no-spin boundary conditions.

2. Basic Equations

The schematic diagram of incompressible laminar flow of micropolar in lid driven square cavity depicted in figure.1a with dimensional Cartesian coordinates x and y . The square cavity enclosed with three stationary walls except top wall, the horizontal top wall moving with uniform velocity ($u=u_0$). In micropolar fluid model, two vector fields which are kinematic independent is introduced - one is representing translation velocities while the other represents angular velocities of particles of the fluid, known as micro rotation vector.

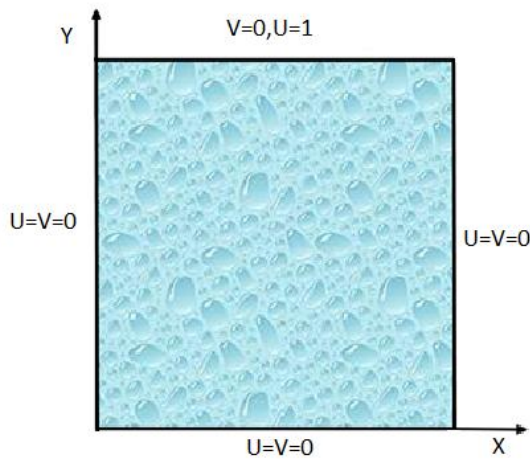


Figure 1a. Physical model.

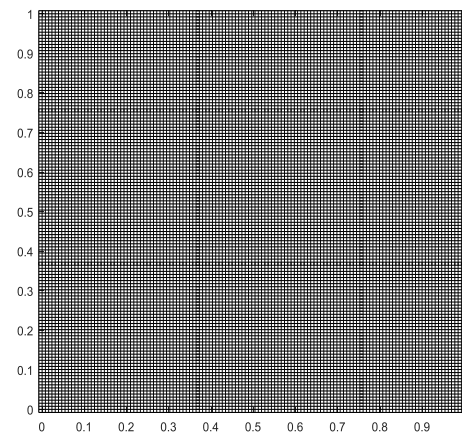


Figure 1b. Uniformly spaced grid. (129X129)

The laminar micro polar fluid and properties of micropolar fluid assumed to be constant except for the variation of density. The governing equations of micropolar fluid flow are taken from Eringen theory of micropolar fluid and are written in dimensional Cartesian form as.

Continuity:

$$\frac{\partial u}{\partial x} + \frac{\partial v}{\partial y} = 0 \quad (1)$$

Momentum:

$$\frac{\partial u}{\partial t} + u \frac{\partial u}{\partial x} + v \frac{\partial u}{\partial y} = -\frac{1}{\rho} \frac{\partial p}{\partial x} + \frac{\mu + k}{\rho} \left(\frac{\partial^2 u}{\partial x^2} + \frac{\partial^2 u}{\partial y^2} \right) + \frac{k}{\rho} \frac{\partial \eta}{\partial y} \quad (2)$$

$$\frac{\partial v}{\partial t} + u \frac{\partial v}{\partial x} + v \frac{\partial v}{\partial y} = -\frac{1}{\rho} \frac{\partial p}{\partial y} + \frac{\mu + k}{\rho} \left(\frac{\partial^2 v}{\partial x^2} + \frac{\partial^2 v}{\partial y^2} \right) - \frac{k}{\rho} \frac{\partial \eta}{\partial x} \quad (3)$$

Angular Momentum:

$$\frac{\partial \eta}{\partial t} + u \frac{\partial \eta}{\partial x} + v \frac{\partial \eta}{\partial y} = \frac{\gamma}{\rho j} \left(\frac{\partial^2 \eta}{\partial x^2} + \frac{\partial^2 \eta}{\partial y^2} \right) - \frac{2k}{\rho j} \eta + \frac{k}{\rho} \left(\frac{\partial v}{\partial x} - \frac{\partial u}{\partial y} \right) \quad (4)$$

Where $\gamma = \left(\mu + \frac{k}{2}\right)j$

Using the appropriate dimensionless quantities

$$X = \frac{x}{L}, Y = \frac{y}{L}, U = \frac{u}{u_0}, \text{Re} = \frac{u_0 L}{\nu}, V = \frac{v}{u_0}, N = \frac{L\eta}{u_0},$$

$$\tau = \frac{u_0 t}{L}, P = \frac{P}{\rho u_0^2}, K = \frac{k}{\mu}, L^2 = j \quad (5)$$

The above governing equations reduced as follows with help of (5)

$$U_x + V_y = 0 \quad (6)$$

$$\frac{DU}{D\tau} = -P_x + (1+K) \frac{1}{\text{Re}} \nabla^2 U + K \frac{1}{\text{Re}} N_y \quad (7)$$

$$\frac{DV}{D\tau} = -P_y + (1+K) \frac{1}{\text{Re}} \nabla^2 V - K \frac{1}{\text{Re}} N_x \quad (8)$$

$$\frac{DN}{D\tau} = \left(1 + \frac{K}{2}\right) \frac{1}{\text{Re}} \nabla^2 N - \frac{2K}{\text{Re}} N + K \frac{1}{\text{Re}} (V_x - U_y) \quad (9)$$

$$\text{Where } \frac{D\phi}{D\tau} = \frac{\partial\phi}{\partial\tau} + U \frac{\partial\phi}{\partial X} + V \frac{\partial\phi}{\partial Y}$$

Stream function and vorticity defined as:

$$U - \frac{\partial\psi}{\partial Y} = 0 \quad V + \frac{\partial\psi}{\partial X} = 0 \quad \frac{\partial V}{\partial X} - \frac{\partial U}{\partial Y} - \omega = 0 \quad (10)$$

Differentiating the equations (7) with respect to Y and differentiating with respect to X of the equation (8) respectively then subtracting. The obtained equations with the help of equation (10), we obtain vorticity transport equation yields

$$\omega = - \left(\frac{\partial^2 \psi}{\partial X^2} + \frac{\partial^2 \psi}{\partial Y^2} \right) \quad (11)$$

$$\frac{\partial\omega}{\partial\tau} + \frac{\partial\psi}{\partial Y} \frac{\partial\omega}{\partial X} - \frac{\partial\psi}{\partial X} \frac{\partial\omega}{\partial Y} = \frac{1}{\text{Re}} (1+K) \left(\frac{\partial^2 \omega}{\partial X^2} + \frac{\partial^2 \omega}{\partial Y^2} \right) - \frac{K}{\text{Re}} \left(\frac{\partial^2 N}{\partial X^2} + \frac{\partial^2 N}{\partial Y^2} \right) \quad (12)$$

With the boundary conditions are

$$\tau = 0 \quad U = V = \psi = \omega = N = 0 \quad \text{For } 0 \leq Y \leq 1 \quad 0 \leq X \leq 1$$

$$\tau > 0, \quad U = V = \psi = 0 \quad \omega = -\frac{\partial U}{\partial Y} \quad N = -n \frac{\partial U}{\partial Y} \quad \text{at } Y = 0,$$

$$\psi = 0, U = 1, \quad \omega = -\frac{\partial U}{\partial Y} \quad N = -n \frac{\partial U}{\partial Y} \quad \text{at } Y = 1,$$

$$U = V = \psi = 0, \quad \omega = -\frac{\partial V}{\partial X} \quad N = -n \frac{\partial V}{\partial X} \quad \text{at } X = 0,1$$

It registered for $K = 0$, the Eqs. (9) and (12) illustrates the classical problem of a Newtonian fluid flow of a Lid driven square cavity.

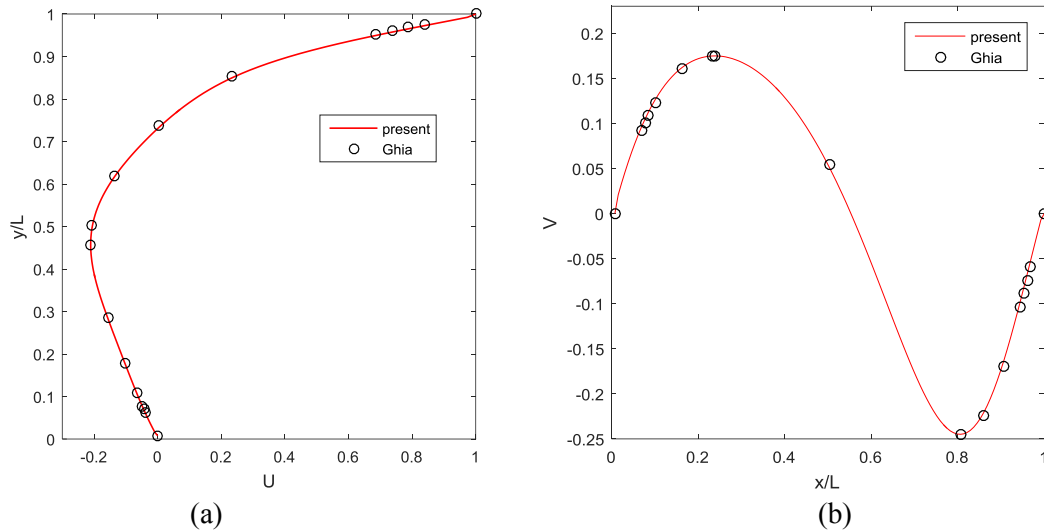


Figure 2. Comparison of Centreline (a) horizontal and (b) vertical velocity for $Re=100$ with mesh system 129×129 .

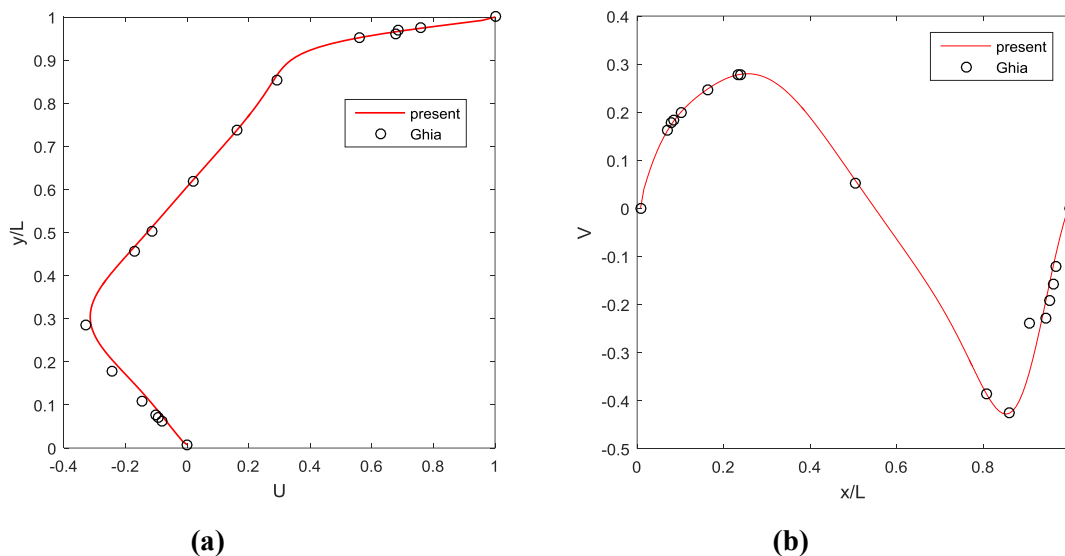


Figure 3. Comparison of Centreline (a) horizontal and (b) vertical velocity for $Re=400$ with mesh system 129×129 .

3. Numerical Method and Validation

In The governing equations (9), (11) and (12) are solved by the method of Euler's explicit technique with appropriate boundary conditions. The poisson's equation of stream function is evaluate by using the Successive over relaxation (SOR) method. Vorticity transport equation and angular momentum equation can be discretized with regular central difference scheme. In order to describe this technique, let us consider the equation (12) as an example. This equation can be re-written as:

$$\frac{\partial \omega}{\partial \tau} + \frac{\partial \psi}{\partial Y} \frac{\partial \omega}{\partial X} - \frac{\partial \psi}{\partial X} \frac{\partial \omega}{\partial Y} = \frac{1}{Re} (1 + K) \left(\frac{\partial^2 \omega}{\partial X^2} + \frac{\partial^2 \omega}{\partial Y^2} \right) - \frac{K}{Re} \left(\frac{\partial^2 N}{\partial X^2} + \frac{\partial^2 N}{\partial Y^2} \right)$$

This equation can be evaluate as follows

$$N\omega = -\frac{\partial\psi}{\partial Y}\frac{\partial\omega}{\partial X} + \frac{\partial\psi}{\partial X}\frac{\partial\omega}{\partial Y} + \frac{1}{\text{Re}}(1+K)\left(\frac{\partial^2\omega}{\partial X^2} + \frac{\partial^2\omega}{\partial Y^2}\right) - \frac{K}{\text{Re}}\left(\frac{\partial^2 N}{\partial X^2} + \frac{\partial^2 N}{\partial Y^2}\right)$$

$$\omega = N\omega + d\tau * \left[-\frac{\partial\psi}{\partial Y}\frac{\partial\omega}{\partial X} + \frac{\partial\psi}{\partial X}\frac{\partial\omega}{\partial Y} + \frac{1}{\text{Re}}(1+K)\left(\frac{\partial^2\omega}{\partial X^2} + \frac{\partial^2\omega}{\partial Y^2}\right) - \frac{K}{\text{Re}}\left(\frac{\partial^2 N}{\partial X^2} + \frac{\partial^2 N}{\partial Y^2}\right) \right]$$

The central difference scheme is used to convective and the diffusion terms. The time integration is applied to the governing equations with time step (dt=0.0001) and ends when time reaches the final level. The procedure is continued in successive time intervals until for the vorticity and the angular velocity converges at a required time when the convergence criteria

$$\frac{|\lambda_{i,j}^{k+1} - \lambda_{i,j}^k|}{|\lambda_{i,j}^{k+1}|} \leq 10^{-6}$$

for vorticity, stream function and angular velocity have been meet. In the above converges criteria k indicates iterative level. The generic variable λ represents ψ , ω and N.

The 2D computation domain is covered by uniform spaced nodes along both X and Y directions and a fine grid of 129X129 is shown in Figure 1b. The numerical code was developed in MATLAB and the present problem for the case of K=0 validated with work of Ghia *et al.* [11] for the values of Re=100 and Re=400. The comparison of centreline velocities of horizontal and vertical velocity profiles are presented in Figures 2&3. These computed results are registered as good agreement. The grid sensitivity test is conducted with uniform spaced grid in Four cases for Re=100: a grid of 69X69 points, a grid of 99X99 points, a grid of 129X129 points and a grid of 159X159 points. **Figure 4** shows an effect of number of grids on horizontal velocity profile along cross-section $X = 0.5$ in the steady state regime. After the verifications of the grid sensitivity, the uniformly spaced grid of 129 X129 points has been taken for the further numerical computation.

The numerical simulation is carried out for the governing parameters: Reynolds number (Re=100, 400, and 1000) and vortex viscosity parameter (K=0.5, 1, 2, 3, 4, and 5), we presents the obtained computation results for the weak concentration case (n = 0). We observed that the case K = 0 shows the fluid is Newtonian. Initially, for this case, computed results are validated with the results of ghia [11] for the square geometry. Particular efforts have been concentrated on the influence of these parameters on lid driven cavity flow. Streamlines and fluid flow rate for various values of dimensionless parameters maintained above are presented in Figures 5-10.

Figure 5 shows the streamlines inside the lid driven square cavity of micropolar fluid with Re=400 and different values of vortex viscosity parameter K. The enlarged clockwise circulation is formed in the middle of the cavity and two anti-clockwise minor circulations are developed at corners of the bottom wall for K=0.5. The influence of vortex viscosity parameter K=1 on fluid flow, the major cell is slight moving towards the top wall is noticed. The considerable changes are observed on minor eddies and the large eddy developed fully inside the cavity by driven top wall with constant velocity for K=2&3. The developed fluid flow patterns are changes inside the cavity for increasing vortex viscosity parameter K. The large clockwise circulation moves towards the top wall and the minor anti-clockwise cells are shrinks with the increasing of vortex viscosity parameter K from k=4 to K=5 is observed. The fluid flow patterns are spread throughout the cavity and the circulation forms at near the top wall is notice at K=5. The mid-section velocity of U are presented in Figure 6 with various values of vortex viscosity parameter K for the Reynolds number Re=400. The minimum value of the U velocity gradually decreases with increasing of vortex viscosity parameter and the fluid particle velocity changes along from bottom to top of the cavity, the major changes are found in middle of the cavity.

The influence of different values of K on mid-section velocity profile V is depicted in Figure 7 with the fixed Reynolds number $Re=400$. The fluid particle velocity decreases when vortex viscosity parameter enhanced. The vortex viscosity parameter ($K=5$) influence on streamlines for $Re=100$ and $Re=1000$ are presented in Figure 8. The major circulation is developed at moving top wall and the minor eddies are diminishes with the affected by vortex viscosity parameter K for $Re=100$. The size of minor eddies are shrinks and the flow patterns are occupies fully inside the cavity for the case of $Re=1000$ with the vortex viscosity parameter K influence. The influence of various values of Reynolds number on micropolar fluid flow velocity profiles are illustrates Figure 9 and Figure 10. The fluid flow particles velocities is observed for $Re=100, 400$ and 1000 with fixed $K=5$. The velocity profiles are increases with the increasing of Reynolds number.

4. Conclusions

In the present paper, unsteady micropolar fluid inside a lid-driven cavity under the influence of vortex viscosity parameter was studied. The Euler's explicit technique was used to compute for the solution of the nonlinear coupled partial differential equations. Comparisons was conducted with published work done by the Newtonian fluid and notice to be in good agreement. The graphical representation results were depicted and discussed. From this numerical investigation, the following conclusions can be drawn.

- The developed minor eddies at corners of bottom wall are diminishes when increasing vortex viscosity parameter K .
- The formation of circular cell drag towards centre of the top wall was predicted when increasing the non-dimensional vortex viscosity parameter.
- The rate of fluid particle motions are increased by the reducing the vortex viscosity parameter.
- The centreline velocity profiles are enhanced with increased Reynolds numbers Re .

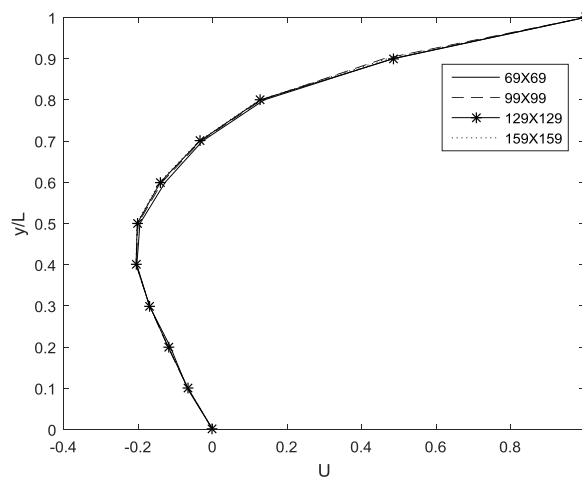


Figure 4. Centreline horizontal velocity profile for different mesh parameters with $Re=100$.

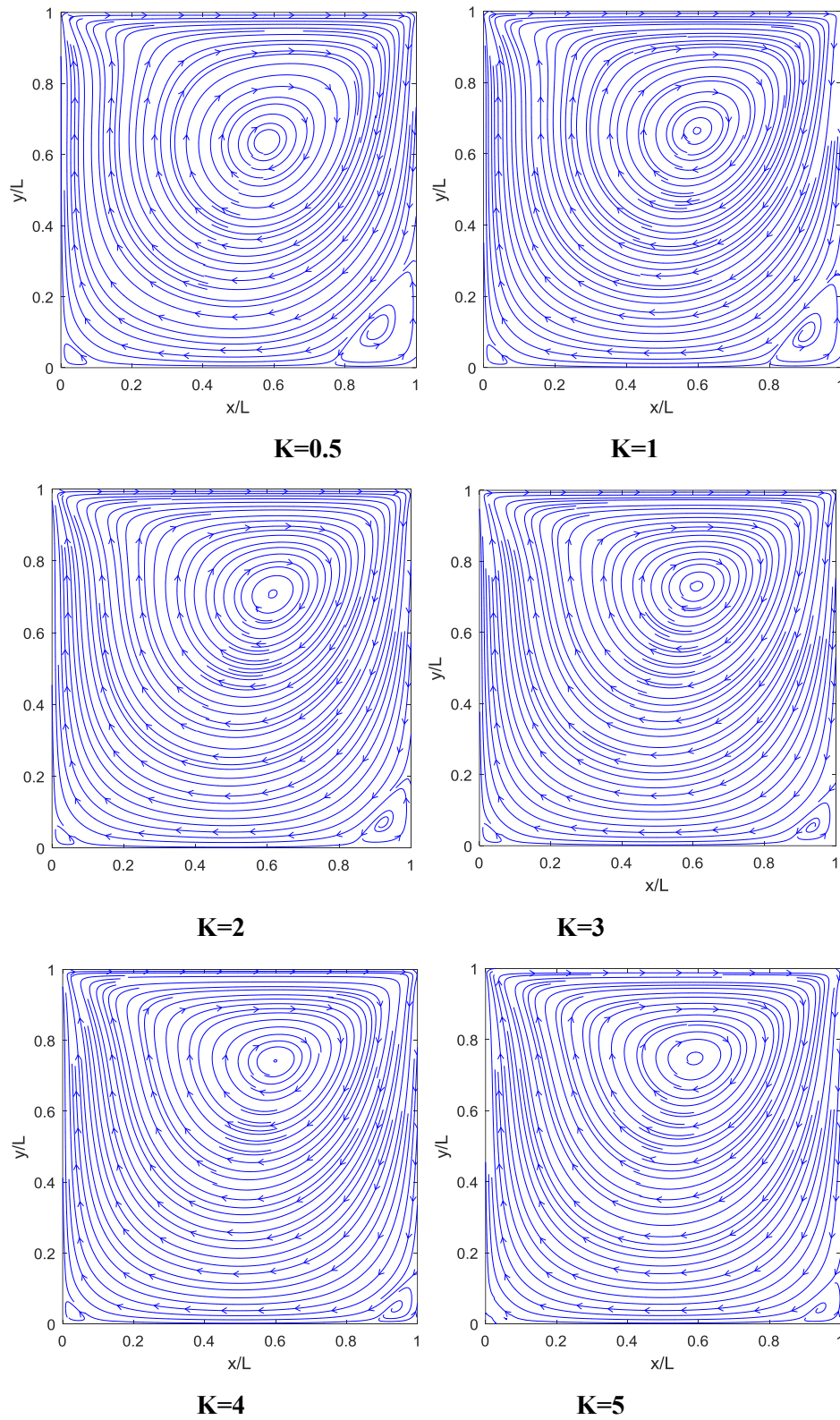


Figure 5. The vortex viscosity parameter K influence on streamlines for $Re=400$.

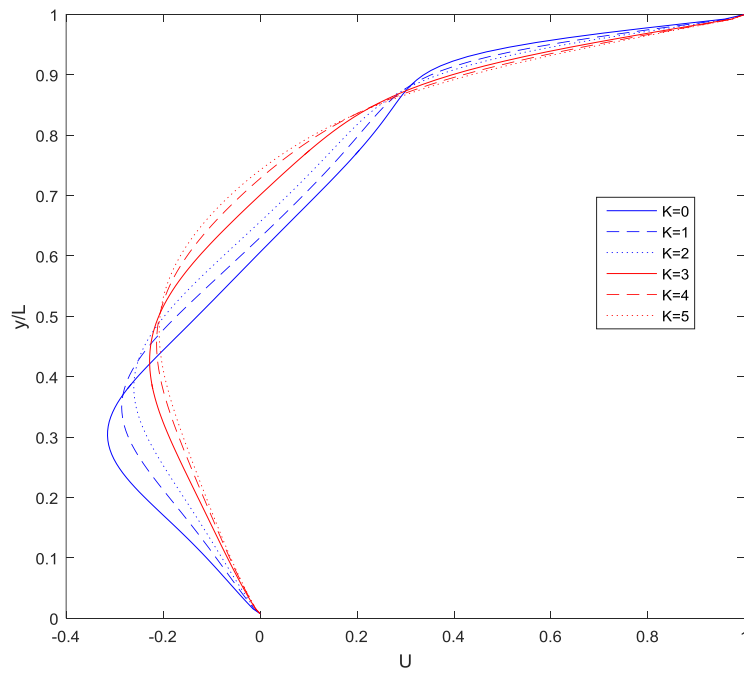


Figure 6. The Influence of vortex viscosity parameter K on mid-section horizontal velocity profile for $Re=400$.

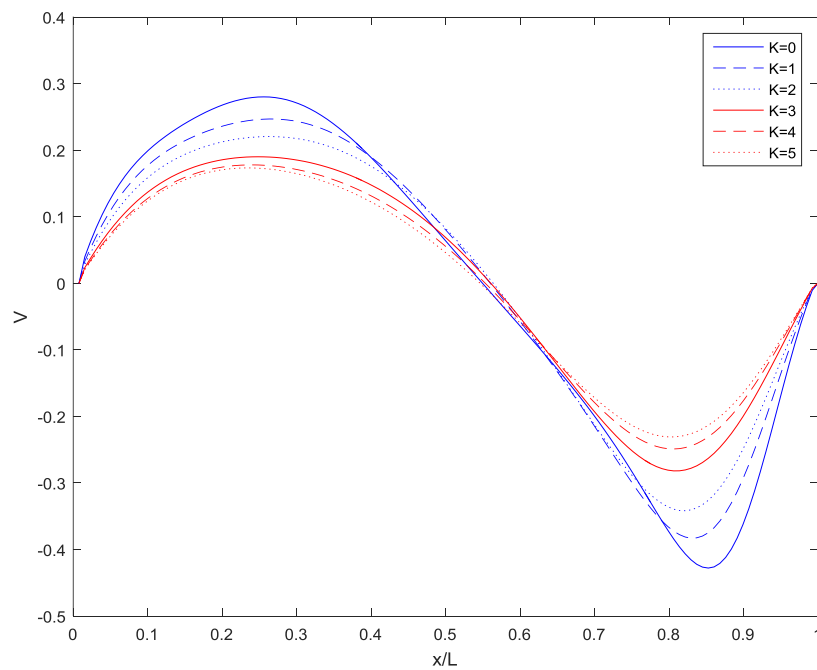


Figure 7. In Influence of vortex viscosity parameter K on mid-section vertical velocity profile for $Re=400$.

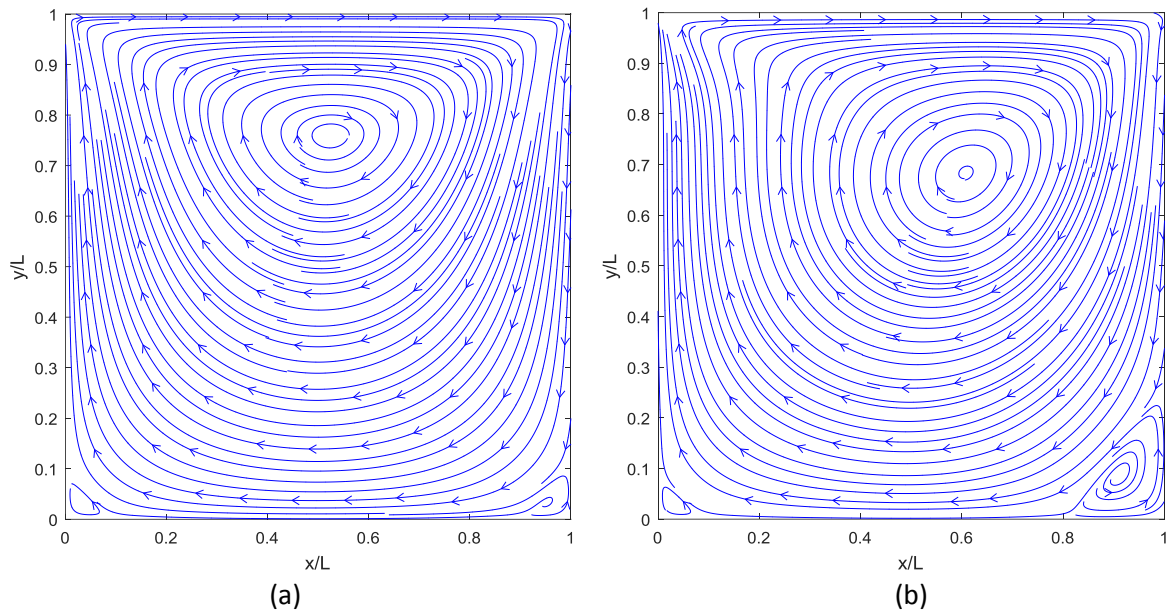


Figure 8. The Reynolds number influence on streamlines for $K=5$ (a) $Re=100$ (b) $Re=1000$.

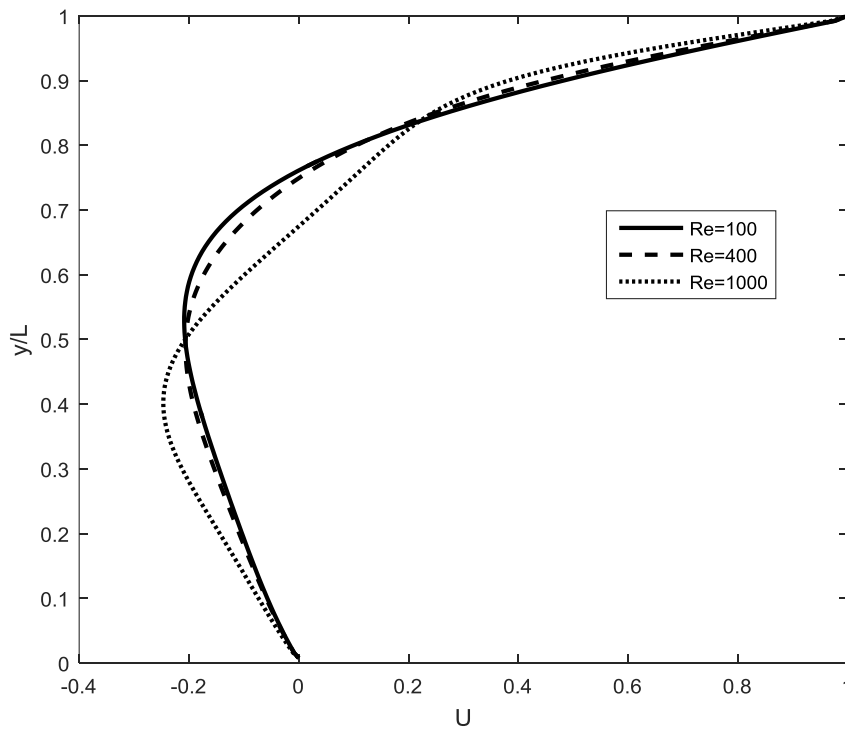


Figure 9. The Reynolds number influence on U-velocity for vortex viscosity parameter $K=5$.

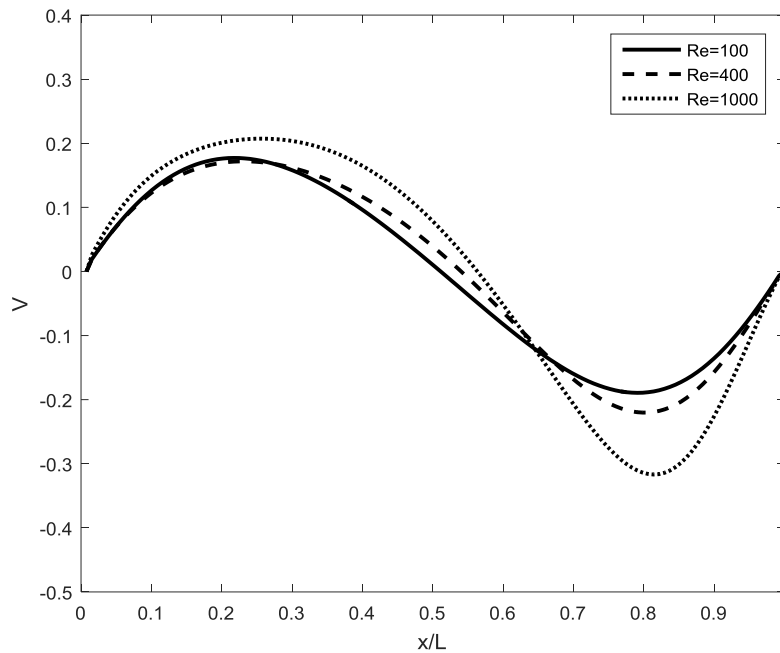


Figure 10. The effect of Reynolds number on V-velocity for $K=5$.

NOMENCLATURE

j = micro-inertia density

K = dimensionless vortex viscosity

k = vortex viscosity

L = enclosure length

n = micro-gyration parameter

N = non-dimensional micro rotation angular velocity

p = pressure

P = non-dimensional pressure

Re = Reynolds number

t = time

u_0 = Lid velocity

(U, V) = dimensionless velocity fields

(u, v) = dimensional velocity profiles

(X, Y) = dimensionless coordinate axes

(x, y) = dimensional coordinate axes

GREEK SYMBOLS

γ = spin-gradient viscosity

ω = dimensionless vorticity

ρ = fluid density

τ = dimensionless time

μ = dynamic viscosity

η = dimensional angular momentum

ψ = stream function

5. References

- [1] Eringen A C 1966 *J. Math. Mech.* **16**, No.1 1-16.
- [2] Arun S, Satheesh A, 2015 *Alexandria Engineering Journal.* **54**, 795–806.
- [3] Nicoleta – Octavia Tanase, Stefan-Mugur Simionescu, Diana Broboana and Corneliu Balan 2017 *Energy Procedia.* **112**, 210 – 216.
- [4] Botella O and Peyreti R 1998 *Computers & Fluids.* **27**, (4) 421-433.
- [5] Santhosh Kumar D, Suresh Kumar K and Manab Kumar Das 2009 *Engineering Applications of Computational Fluid Mechanics.* **3**(3), 336–354.
- [6] Erturk E, Corke T C and Gokcol C 2005 *International journal for numerical methods in fluids,* **48**, 747-774.
- [7] Moojlt A, Burley D, Rawson H 1997 *International journal for numerical methods in engineering.* **14**, 11-35.
- [8] Massarotti N, Arpino F, Lewis R W and Nithiarasu P 2006 *International journal for numerical methods in engineering.* **66**, 1618-1640.
- [9] Sandrine hugues and anthony Randriamampianina 1998 *International journal for numerical methods in fluids.* **28**, 501-521.
- [10] Zhenquan Li, Robert Wood 2015 *Journal of Computational and Applied Mathematics.* **275**, 262-271.
- [11] Ghia U, Ghia K N and C.T. Shin 1982 *Journal of Computational Physics.* **48**, 387–411.
- [12] Harry A, Hogan, Mogens Henriksen 1989 *Journal of Biomechanics.* **22**(3), 211-218.
- [13] Sherief H H, Faltas M S, Ashmawya E A, Abdel-Hameid A M 2016 *European Journal of Mechanics B/Fluids.* **59**, 186–196.
- [14] Hari R. Kataria, Harshad R. Patel, Rajiv Singh 2017 *Ain Shams Engineering Journal.* **8**, 87–102.
- [15] James Chen, James D. Lee, Chunlei Liang 2011 *Journal of Non-Newtonian Fluid Mechanics.* **166**, 867–874.
- [16] Ettwein F, Růžička M, Weber B 2015 *Nonlinear Analysis.* **125**, 1–29.
- [17] Muthu P, Rathish kumar B V and Peeyush Chandra 2008 *Journal of Mechanics in Medicine and Biology.* **8**(4), 561-576.
- [18] Hogan H A, Henriksen M 1991 *International journal for numerical methods in fluids.* **13**, 1267-1287.